PNAS

Supplementary Information for

Endothelial VWF is critical for the pathogenesis of vaso-occlusive episode in a mouse model of sickle cell disease

Huiping Shi[a,b], Bojing Shao[a], Liang Gao[a], Thamizh Venkatesan[a], John Michael McDaniel[a], Meixiang Zhou[a], Samuel McGee[a], Pengchun Yu[a], Jasimuddin Ahamed[a], Janna Journeycake[c], James N. George[d], and Lijun Xia[a,b,1]

[a]Cardiovascular Biology Research Program, Oklahoma Medical Research Foundation, Oklahoma City, OK, 73104, USA. [b]Department of Biochemistry and Molecular Biology, University of Oklahoma Health Sciences Center, Oklahoma City, OK, 73104, USA. [c]Hematology-Oncology Section, Department of Pediatrics, University of Oklahoma Health Sciences Center, Oklahoma City, OK, 73104, USA. [d]Hematology-Oncology Section, Department of Medicine, University of Oklahoma Health Sciences Center, Oklahoma City, OK, 73104, USA.

[1]To whom correspondence may be addressed.

Lijun Xia, M.D., Ph.D., Cardiovascular Biology Research Program, Oklahoma Medical Research Foundation, 825 N.E. 13th Street, Oklahoma City, OK 73104; Phone: 405-271-7892. Fax: 405-271-3137. Email: lijun-xia@omrf.org

This PDF file includes:

Supplementary Figures S1 to S11
Legends for Movies S1 to S3

Other supplementary materials for this manuscript include the following:

Movies S1 to S3

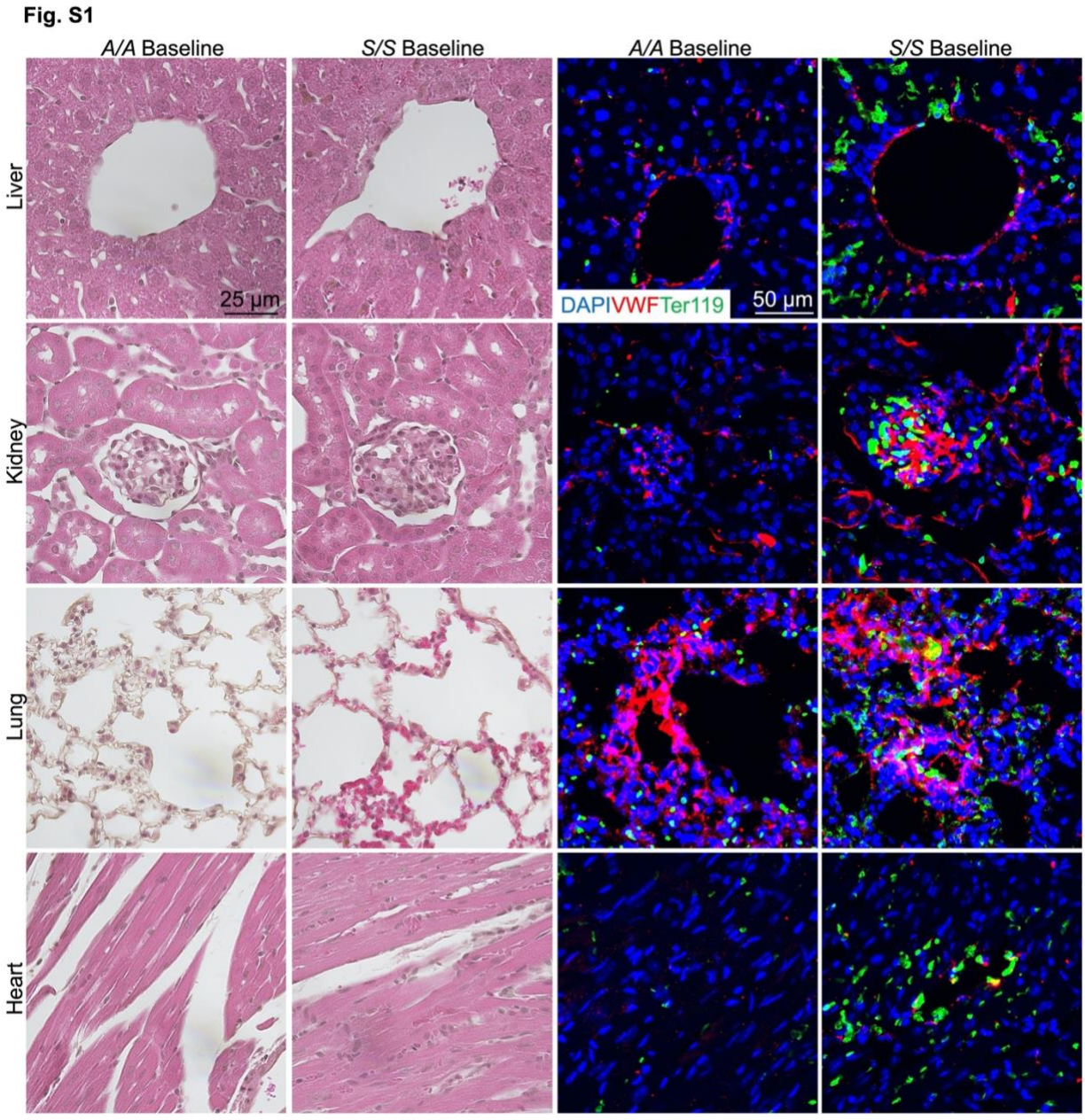

Fig. S1. Histology analysis and immunofluorescence staining of tissues collected from *A/A* and *S/S* mice at baseline. Representative images of H&E-stained paraffin sections for liver, kidney, lung, and heart collected from *A/A* and *S/S* mice at baseline were shown on the left (scale bar: 25 μm). Representative immunofluorescence images of liver, kidney, lung, and heart collected from *A/A* and *S/S* mice at baseline were shown on the right (scale bar: 50 μm). Slides were stained with primary antibodies to VWF and red blood cells (Ter119). DAPI, cell nuclear staining. n = 4 mice per genotype.

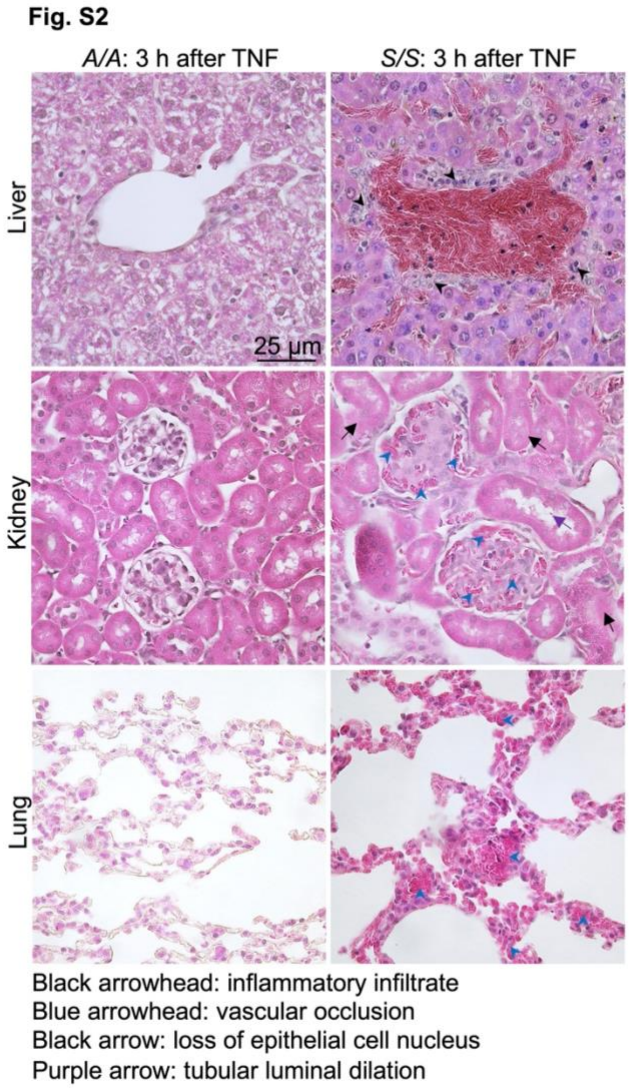

Fig. S2. Pathological changes of liver, kidney, and lung from *S/S* mice relative to that from *A/A* mice at 3 h after VOE induction. VOE was induced by intraperitoneal injection of 500 ng TNF. Representative images of H&E-stained paraffin sections for liver, kidney, and lung collected from *A/A* and *S/S* mice at 3 h after VOE induction were shown. Scale bar: 25 μm. Black arrowhead indicates inflammatory infiltrate. Blue arrowhead indicates vascular occlusion. Black arrow indicates loss of epithelial cell nucleus. Purple arrow indicates tubular luminal dilation. n = 4 mice per genotype.

Fig. S3

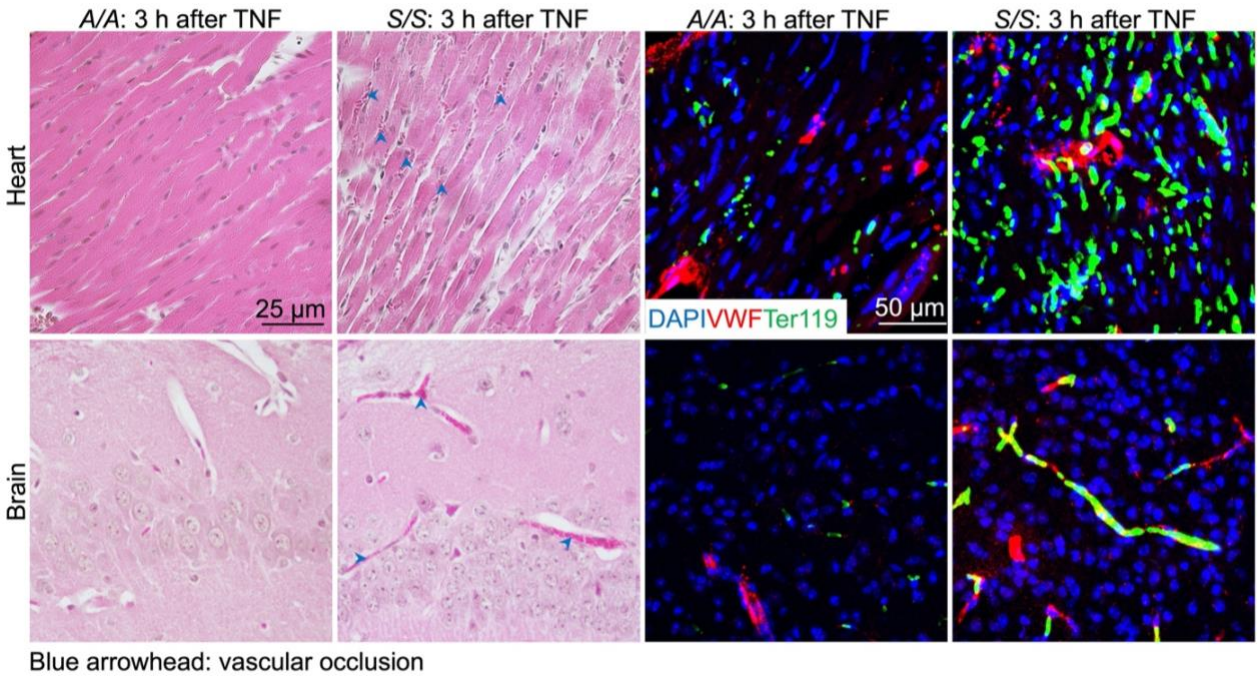

Fig. S3. Pathological changes and immunofluorescence staining results of heart and brain collected from *S/S* mice relative to that from *A/A* mice at 3 h after VOE induction. VOE was induced by intraperitoneal injection of 500 ng TNF. Representative images of H&E-stained paraffin sections for heart and brain collected from *A/A* and *S/S* mice at 3 h after VOE induction were shown on the left (scale bar: 25 μm). Blue arrowhead indicates vascular occlusion. Representative immunofluorescence images of heart and brain collected from *A/A* and *S/S* mice at 3 h after VOE induction were shown on the right (scale bar: 50 μm). Slides were stained with primary antibodies to VWF and red blood cells (Ter119). DAPI, cell nuclear staining. n = 4 mice per genotype.

Fig. S4

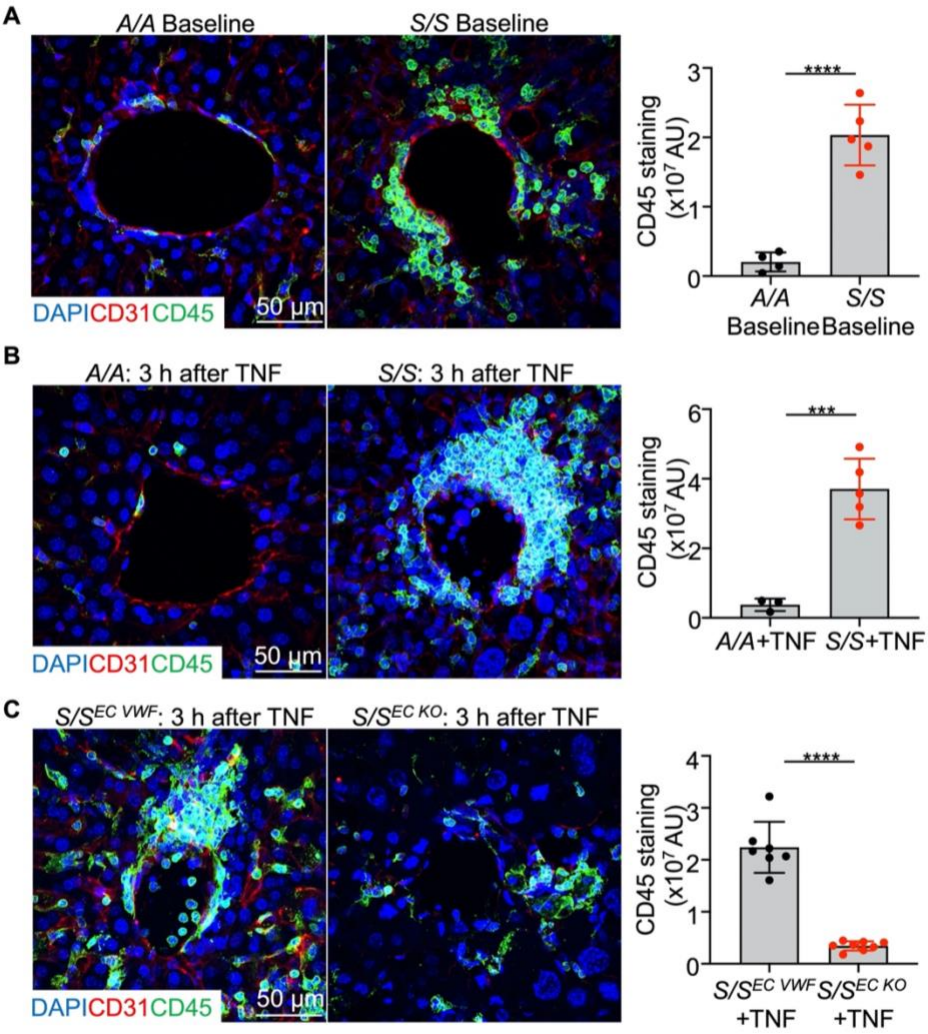

Fig. S4. Comparison of liver inflammatory infiltrates at baseline and 3 h after VOE induction. Mouse tissues were collected from *A/A* and *S/S* mice at baseline (*A*), as well as *A/A*, *S/S* (*B*), $S/S^{EC\ VWF}$, and $S/S^{EC\ KO}$ (*C*) mice at 3 h after TNF-induced VOE. Liver cryo-sections were stained with primary antibodies to CD31 (endothelial marker) and CD45 (marker of inflammatory cells). DAPI, cell nuclear staining. Quantification of CD45 staining was shown on the right. AU: arbitrary unit. Scale bar, 50 µm. n = 4 mice per genotype. Data represent mean ± standard deviation. ***, $P < 0.001$; ****, $P < 0.0001$, two tailed, unpaired Student's t-test.

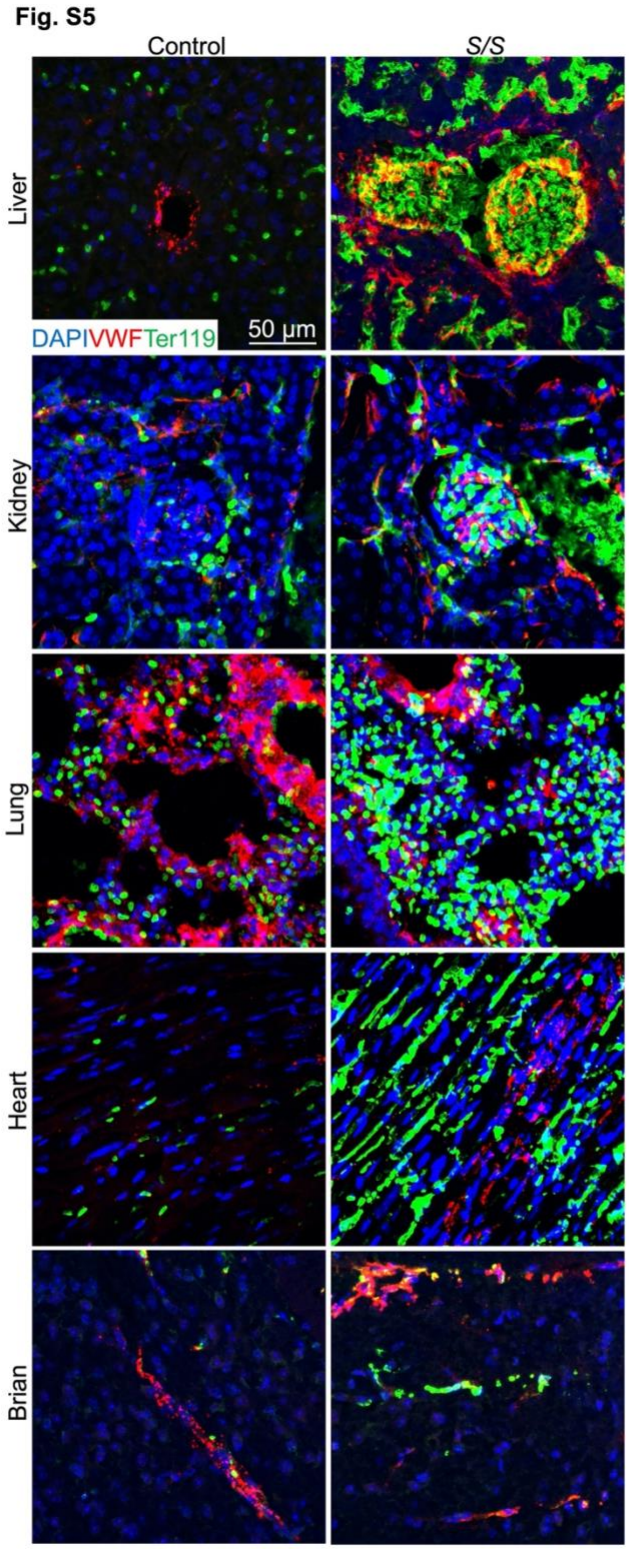

Fig. S5. Representative immunofluorescence images of liver, kidney, lung, heart, and brain cryo-sections from control and SCD mice after hypoxia/reoxygenation-induced VOE. VOE was induced by challenging mice with hypoxia (8% O_2) for 10 hours followed by reoxygenation for 2

hours. Slides were stained with primary antibodies to VWF and red blood cells (Ter119). DAPI, cell nuclear staining. Scale bar: 50 μm.

Fig. S6

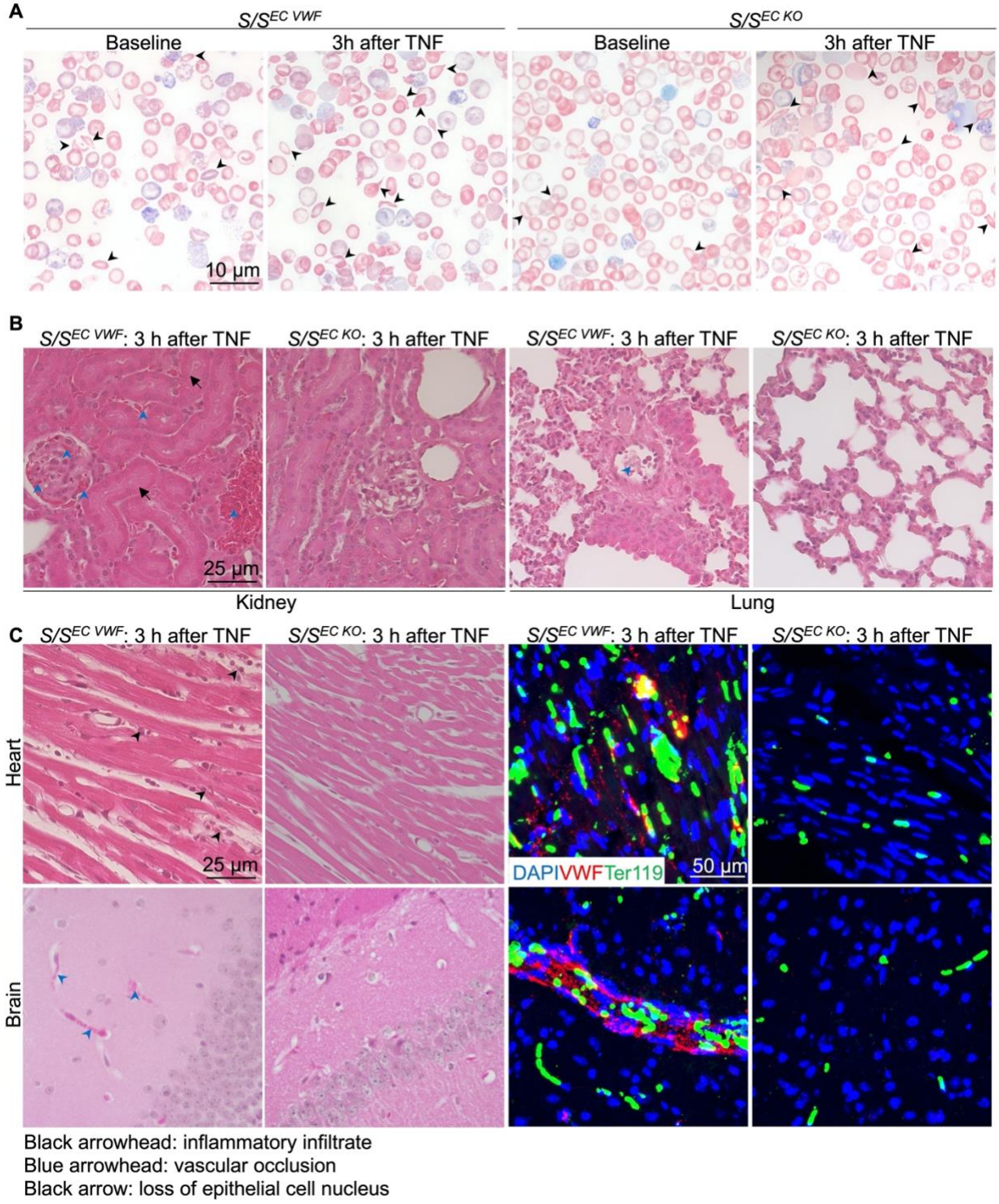

Fig. S6. Blood smear and histopathological analysis of *S/S*$^{EC\ VWF}$ and *S/S*$^{EC\ KO}$ mice. (*A*) Blood smear performed before and after VOE induction for *S/S*$^{EC\ VWF}$ and *S/S*$^{EC\ KO}$ mice. Arrowheads indicate sickle red blood cells. Scale bar: 10 μm. (*B*) Representative images of H&E-stained paraffin sections of kidney and lung collected from *S/S*$^{EC\ VWF}$ and *S/S*$^{EC\ KO}$ mice at 3 h after VOE induction. Scale bar: 25 μm. n = 5 mice per genotype. (*C*) Representative images of H&E-stained

paraffin sections (scale bar: 25 μm) and representative immunofluorescence images (scale bar: 50 μm) of heart and brain collected from *S/S*$^{EC\ VWF}$ and *S/S*$^{EC\ KO}$ mice at 3 h after VOE induction. Black arrowhead indicates inflammatory infiltrate. Blue arrowhead indicates vascular occlusion. Black arrow indicates loss of epithelial cell nucleus. Cryosections were stained with primary antibodies against VWF and red blood cells (Ter119). DAPI, cell nuclear staining. n = 5 mice per genotype.

Fig. S7

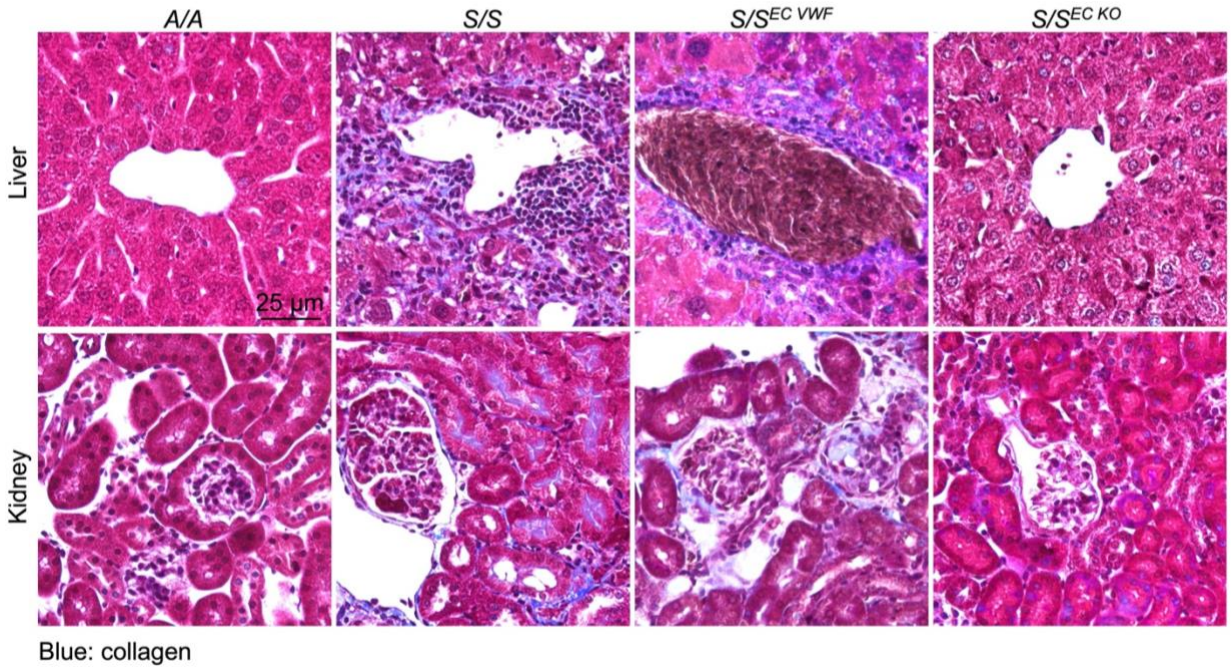

Fig. S7. Trichrome staining of liver and kidney collected from *A/A*, *S/S*, *S/S*$^{EC\ VWF}$ and *S/S*$^{EC\ KO}$ mice. Scale bar: 25 µm. Blue color indicates collagen deposition. n = 4 mice per group.

Fig. S8

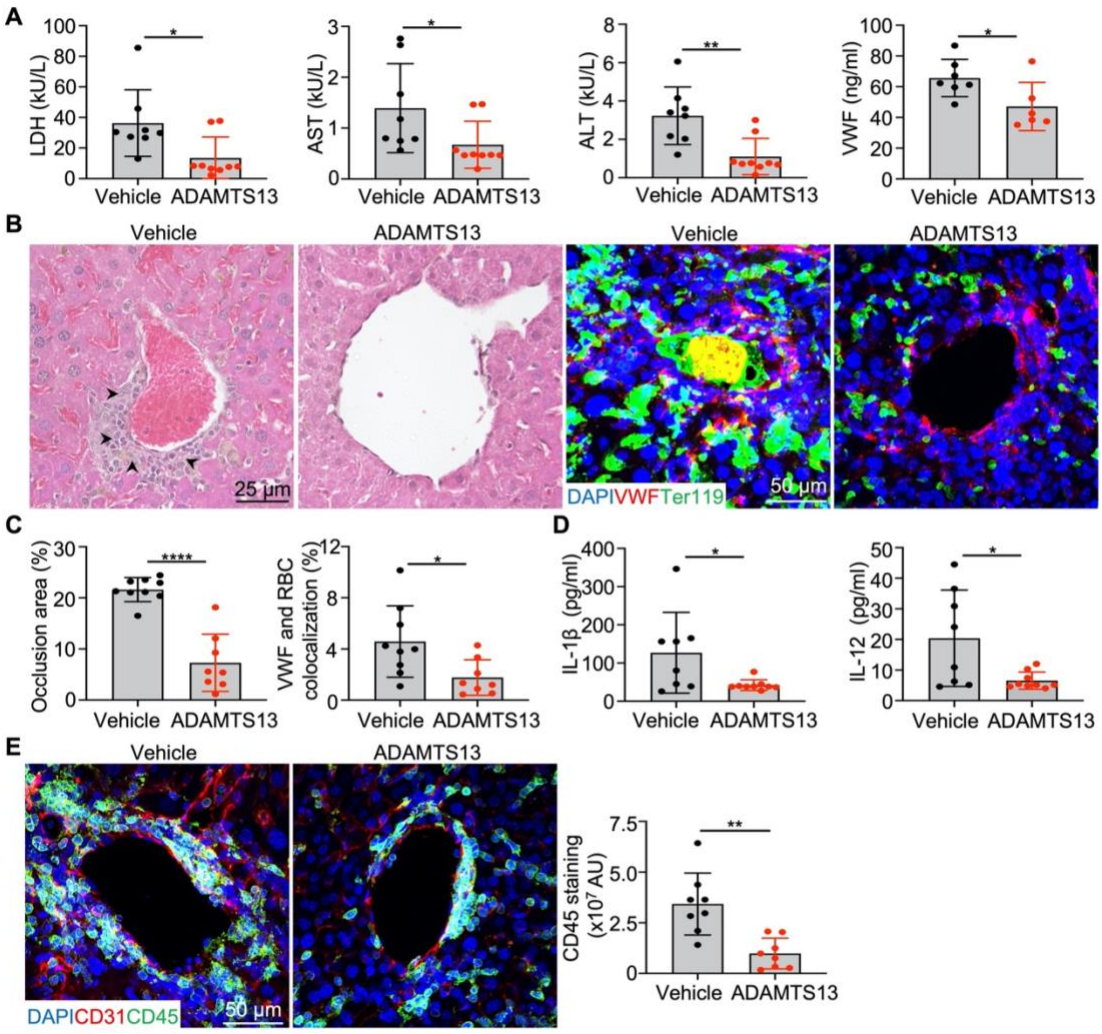

Fig. S8. ADAMTS13 injection before VOE improves histopathological phenotypes of VOE in SCD mice. (*A*) Plasma levels of LDH, AST, ALT, and VWF in vehicle- or ADAMTS13-pre-treated *S/S* mice after TNF-induced VOE. Each dot represents one mouse. Data represent mean ± standard deviation. **P* < 0.05; ***P* < 0.01, Mann-Whitney test for LDH comparison and two tailed, unpaired Student's t-test for other comparisons. (*B*) Representative images of H&E-stained paraffin sections and representative immunofluorescence images of cryo-sections of liver collected from vehicle- or ADAMTS13-pre-treated *S/S* mice after TNF-induced VOE. H&E-stained liver paraffin sections showed reduced vaso-occlusion and inflammatory cell infiltration (indicated by arrowheads) in ADAMTS13-pre-treated *S/S* mice when compared to vehicle-pre-treated *S/S* mice. Scale bar: 25 µm. Cryo-sections were stained with primary antibodies to VWF and red blood cells (Ter119). DAPI, cell nuclear staining. There was decreased VWF-rich vaso-occlusion in ADAMTS13-pre-treated *S/S* mice when compared to vehicle-pre-treated *S/S* mice. Scale bar, 50 µm. n = 5 mice per treatment group. (*C*) Quantification of vaso-occlusion by sickle red blood cells and co-localization (yellow) of VWF with sickle red blood cells (Ter119) in (*B*). Data represent mean ± standard deviation. **P* < 0.05; *****P* < 0.0001, two tailed, unpaired Student's t-test. (*D*) Quantification of post-induction plasma cytokine levels of vehicle- or

ADAMTS13-pre-treated *S/S* mice by ELISA. Each dot represents one mouse. Data represent mean ± standard deviation. **P* < 0.05, Mann-Whitney test for IL-1β comparison and two tailed, unpaired Student's t-test for IL-12 comparison. (*E*) Representative immunofluorescence images of cryo-sections of liver collected from vehicle- or ADAMTS13-pre-treated *S/S* mice after TNF-induced VOE. Cryo-sections were stained with primary antibodies to CD31 and CD45. DAPI, cell nuclear staining. Quantification of CD45 was shown on the right and there was reduced inflammatory cell infiltration in ADAMTS13-pre-treated *S/S* mice when compared to vehicle-treated *S/S* mice. Scale bar, 50 μm. n = 5 mice per treatment group. Data represent mean ± standard deviation. ***P* < 0.01, two tailed, unpaired Student's t-test.

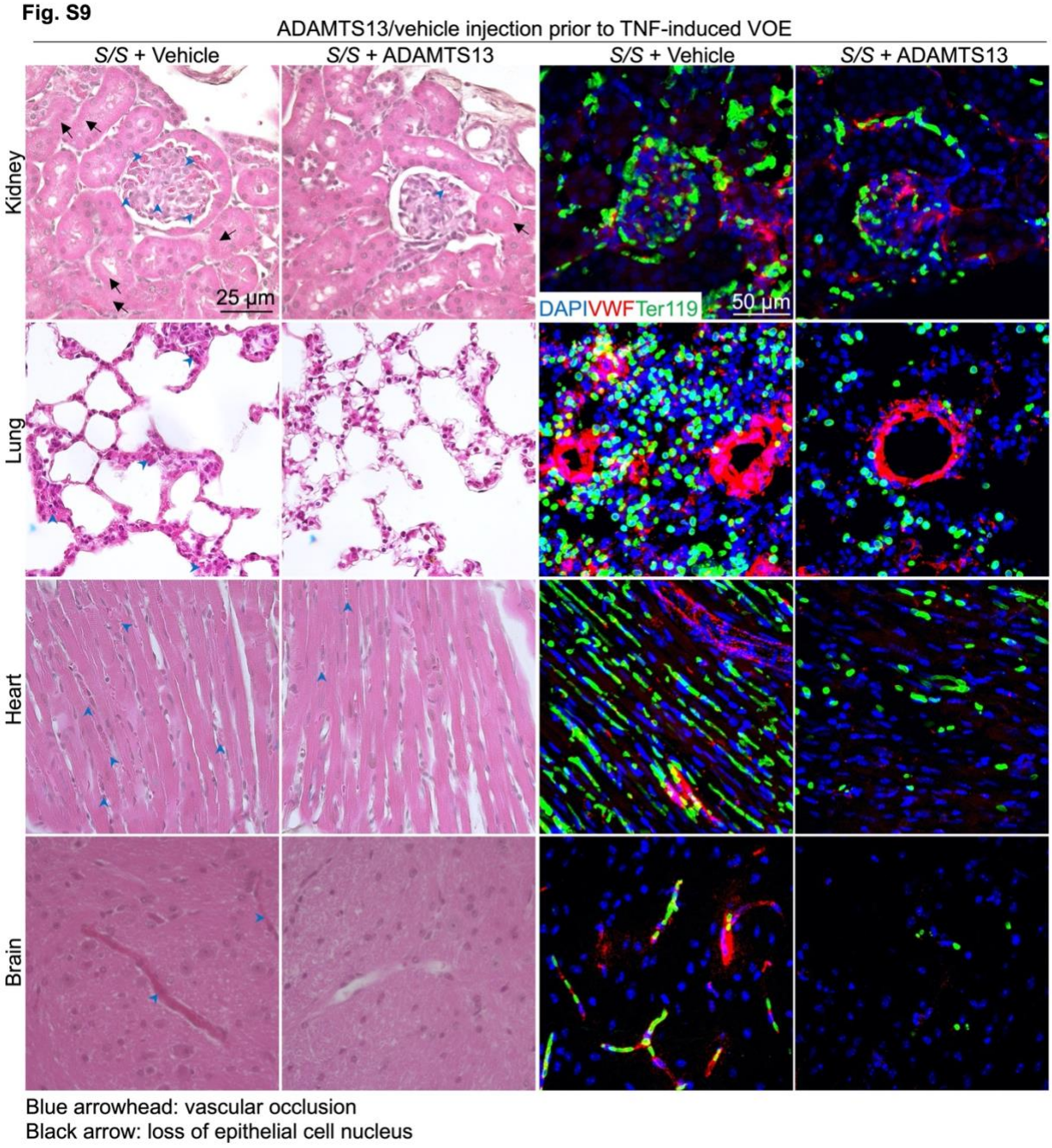

Fig. S9. Histology analysis and immunofluorescence staining of tissues collected from vehicle- or ADAMTS13-pre-treated *S/S* mice at 3 h after VOE induction. *S/S* mice were pre-treated with ADAMTS13 or same volume of vehicle 15 min before VOE induction. VOE was induced by intraperitoneal injection of 500 ng TNF. Representative images of H&E-stained paraffin sections for kidney, lung, heart, and brain collected from vehicle- or ADAMTS13-pre-treated *S/S* mice at 3 h after VOE induction were shown on the left (scale bar: 25 μm). Blue arrowhead indicates vascular occlusion. Black arrow indicates loss of epithelial cell nucleus. Representative immunofluorescence images of kidney, lung, heart, and brain collected from vehicle- or ADAMTS13-pre-treated *S/S* mice at 3 h after VOE induction were shown on the right (scale bar:

50 μm). Slides were stained with primary antibodies to VWF and red blood cells (Ter119). DAPI, cell nuclear staining. n = 5 mice per treatment group.

Fig. S10

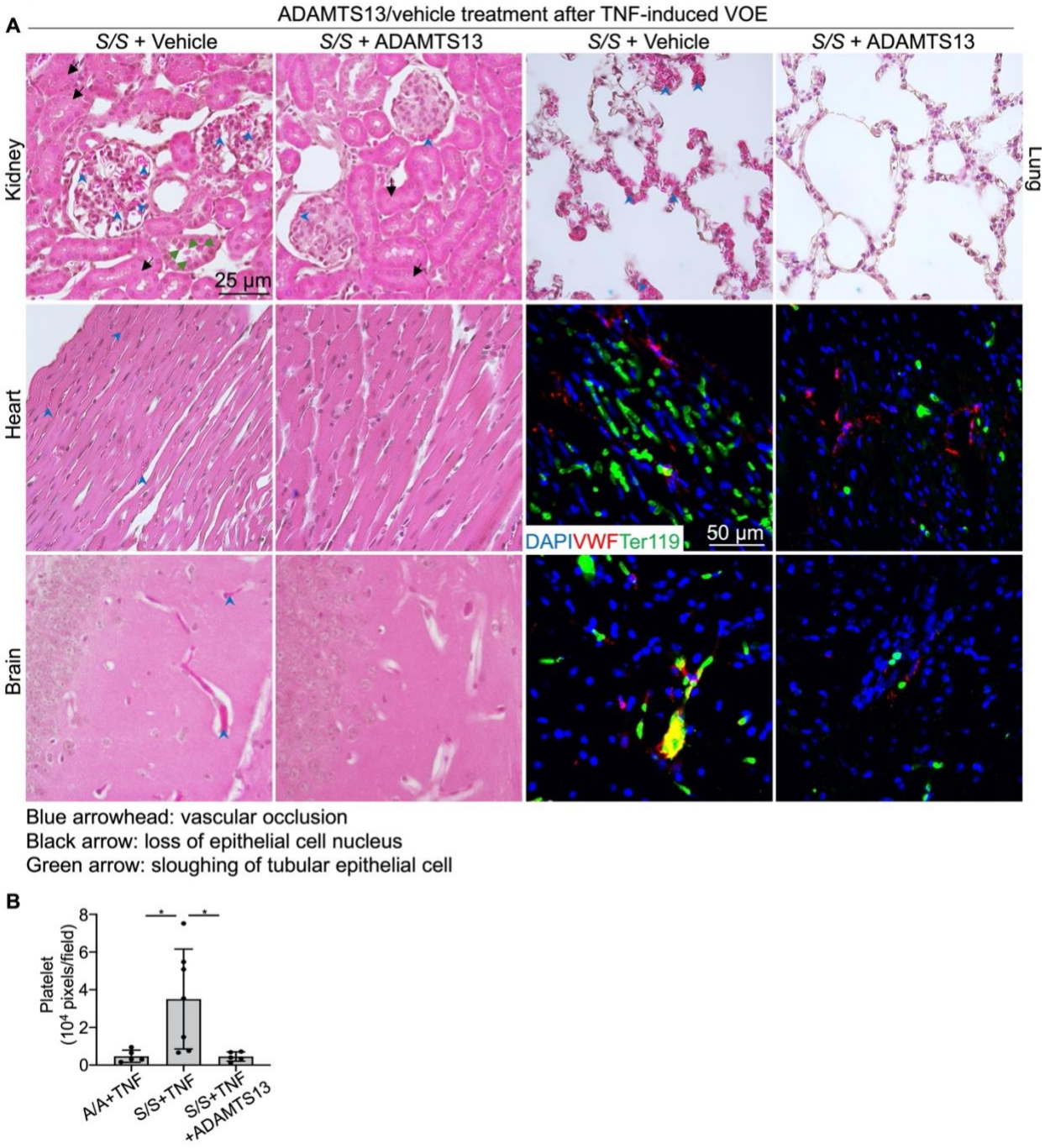

Fig. S10. Histology analysis and immunofluorescence staining of tissues collected from vehicle- or ADAMTS13-treated *S/S* mice at 3 h after VOE induction. (*A*) VOE was induced by intraperitoneal injection of 500 ng TNF. After 15 min, *S/S* mice were treated with ADAMTS13 or same volume of vehicle. Representative images of H&E-stained paraffin sections for kidney, lung, heart, and brain collected from vehicle- or ADAMTS13-treated *S/S* mice at 3 h after VOE induction were shown (scale bar: 25 μm). Blue arrowhead indicates vascular occlusion. Black arrow indicates loss of epithelial cell nucleus. Green arrow indicates sloughing of tubular epithelial cell. Representative immunofluorescence images of heart and brain collected from

vehicle- or ADAMTS13-treated *S/S* mice at 3 h after VOE induction were shown on the right (scale bar: 50 μm). Slides were stained with primary antibodies to VWF and red blood cells (Ter119). DAPI, cell nuclear staining. n = 5 mice per treatment group. (*B*) Quantification of platelet involvement in vaso-occlusions visualized by intravital spinning disk confocal microscopy real-time imaging. n = 3 mice per genotype. Data represent mean ± standard deviation. *, $P < 0.05$, one-way ANOVA.

Fig. S11

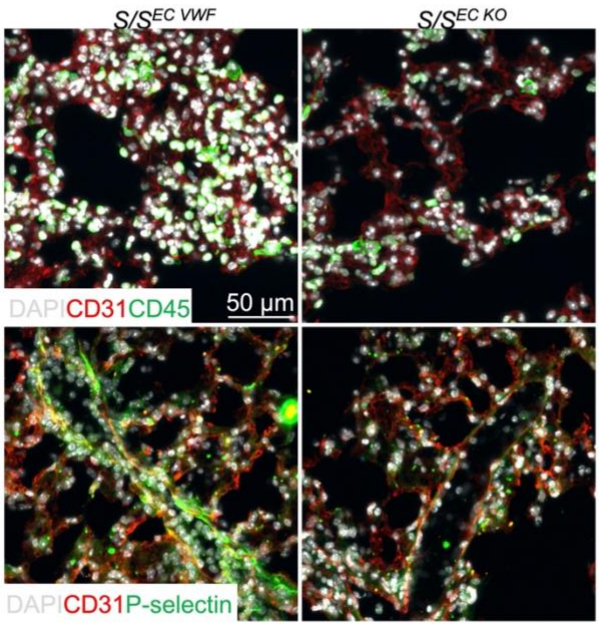

Fig.S11. Reduced inflammatory infiltrates and P-selectin in *S/S*$^{EC\ KO}$ mice. Representative immunofluorescence images of cryo-sections of lungs collected from *S/S*$^{EC\ VWF}$ and *S/S*$^{EC\ KO}$ mice were shown. Lung cryosections were stained with primary antibodies to CD31, CD45 and P-selectin. DAPI, cell nuclear staining. Scale bar: 50 µm. n = 4 mice per genotype.

Movie S1. A representative video clip of intravital spinning disk confocal microscopy real-time imaging of liver sinusoidal blood flow in *A/A* mice after TNF challenge. *A/A* mice were intravenously injected with fluorophore-conjugated antibody specific to either red blood cells (Ter119, red), platelets (CD41, green), or endothelial cells (CD31, blue) after TNF challenge. Unobstructed blood flow was seen in the liver sinusoids of *A/A* mice after TNF challenge. Frame rate = 5 fps. Data represent results of three *A/A* mice after TNF challenge.

Movie S2. A representative video clip of intravital spinning disk confocal microscopy real-time imaging of vaso-occlusion in *S/S* mice with TNF-induced VOE. *S/S* mice with TNF-induced VOE were intravenously injected with fluorophore-conjugated antibody specific to either red blood cells (Ter119, red), platelets (CD41, green), or endothelial cells (CD31, blue). Vaso-occlusion and adherent platelets were seen in the liver sinusoids. Frame rate = 5 fps. Data represent results of three *S/S* mice with TNF-induced VOE.

Movie S3. A representative video clip of intravital spinning disk confocal microscopy real-time imaging of vaso-occlusion in ADAMTS13-treated *S/S* mice with TNF-induced VOE. ADAMTS13-treated *S/S* mice with TNF-induced VOE were intravenously injected with fluorophore-conjugated antibody specific to either red blood cells (Ter119, red), platelets (CD41, green), or endothelial cells (CD31, blue). Reduced vaso-occlusion and adherent platelets in liver sinusoids were observed after ADAMTS13 treatment of *S/S* mice with TNF-induced VOE. Frame rate = 5 fps. Data represent results of three ADAMTS13-treated *S/S* mice with TNF-induced VOE.